Experimental study of the $^{17}F + ^{12}C$ fusion reaction and its implications for fusion of proton-halo systems

B. W. Asher,* S. Almaraz-Calderon,† Vandana Tripathi, K. W. Kemper, L. T. Baby, N. Gerken, E. Lopez-Saavedra, A. B. Morelock, J. F. Perello, and I. Wiedenhöver
Department of Physics, Florida State University, Tallahassee, Florida 32306, USA

N. Keeley
National Centre for Nuclear Research, ulica Andrzeja Sołtana 7, 05-400 Otwock, Poland

(Received 9 October 2020; revised 2 February 2021; accepted 12 April 2021; published 29 April 2021)

The total fusion cross section for the $^{17}F + ^{12}C$ system at incident energies near the top of the Coulomb barrier was studied using the newly developed *Encore* active-target detector at Florida State University. The ^{17}F nucleus exhibits interesting nuclear structure properties in that although it has a low threshold against $^{17}F \rightarrow ^{16}O + p$ breakup ($S_p = 600$ keV), the valence proton is in the $1d_{5/2}$ shell in the ground state so that the nuclear matter radius is predicted to be similar to that of the ^{16}O core. By contrast, the low-lying $1/2^+$ first excited state (bounded by 105 keV) with the valence proton in the $2\,s_{1/2}$ shell is considered to be a proton halo. In this paper possible influences of both the weak binding and the halo nature of the excited state on the total fusion cross section were investigated. The new data reported here complement existing measurements for the total fusion of ^{17}F with heavy (^{208}Pb) and medium mass (^{58}Ni) targets by extending the range of systems studied to one where Coulomb effects should be minimal. Total fusion cross sections for the stable counterpart systems $^{16}O + ^{12}C$ and $^{19}F + ^{12}C$ were also measured to enable a systematic comparison. No significant influence of either the weak binding or the halo nature of the ^{17}F $1/2^+$ first excited state on the above barrier total fusion excitation function was observed when compared with the stable counterpart systems.

DOI: 10.1103/PhysRevC.103.044615

I. INTRODUCTION

Fusion measurements are a key component of research in nuclear structure, nuclear reactions, and nuclear astrophysics [1]. For example, the $^{12}C + ^{12}C$ fusion reaction determines the burning conditions and subsequent isotopic composition of the resulting ashes in massive stars [2]. Furthermore, in neutron-rich stars fusion of exotic carbon and oxygen isotopes may act as catalyzers for the so-called x-ray superbursts [3]. Recently, fusion reaction experiments involving light exotic beams have become the focus of several studies since such nuclei have become accessible at existing facilities. This area of research will only grow with the forthcoming exotic beam facilities around the world. Beams of short-lived radioactive nuclei present unique opportunities to probe the dynamics of fusion reactions around the Coulomb barrier. Weakly bound light exotic nuclei, in particular, provide the possibility to explore the interplay between fusion, breakup, and transfer reactions over a much wider range of binding energies and structural properties than those available with stable beams [4]. A specific subclass of this type of nucleus are the so-called halo nuclei which have extended matter distributions [5,6] such that large breakup and/or transfer cross sections are observed at incident energies close to the Coulomb barrier [7].

It has long been suggested that the fusion cross section should be significantly enhanced in systems involving halo nuclei [8,9] due to their extended size since the fusion probability is highly dependent on the size and the shape of the interacting nuclei. On the other hand, due to their low threshold against breakup it has also been suggested that there could be significant suppression of fusion in such systems. However, the question of whether or not fusion in systems involving halo nuclei is enhanced has not yet been satisfactorily answered experimentally. In fact, fusion reactions involving halo nuclei have led to contradictory conclusions [4,8–10] which could be the result of experimental uncertainties but also the lack of sufficient data for a systematic comparison between systems. A more fundamental problem is the lack of general agreement as to the benchmark used to infer enhancement or suppression and whether complete fusion or total fusion should be considered (see, e.g., Ref. [4] for a discussion of these questions).

Most experiments with halo nuclei have been carried out on the neutron-rich side of the chart of the nuclides [4]. Results of fusion reactions with the neutron-rich halo nuclei $^{6,8}He$ [11,12], ^{11}Li [13], and ^{11}Be [14,15] show an effect on the fusion excitation function which is mainly manifested as a reduction in the cross section above the barrier. This effect has been explained by the low neutron removal thresholds of these

*bwa15@my.fsu.edu
†salmarazcalderon@fsu.edu

systems [10], resulting in the loss of beam flux at relatively long distances between the colliding nuclei due to breakup itself and/or neutron transfer reactions.

For proton-halo nuclei, despite the expanded size of the halo their weakly bound nature might also be expected to manifest itself as a reduction of the fusion cross section above the Coulomb barrier [10,16]. However, the few available experimental results appear inconsistent. For example, the proton-halo nucleus ^{8}B has been the object of various studies with ^{58}Ni and ^{28}Si [17,18] targets. The $^{8}\mathrm{B}+^{58}\mathrm{Ni}$ system showed an enhancement in the fusion cross section in all regions including well above the Coulomb barrier whereas the $^{8}\mathrm{B}+^{28}\mathrm{Si}$ system shows a slight suppression above the barrier [17,18].

The conclusions concerning the fusion of ^{17}F, the focus of this paper, are also not definitive. The ^{17}F nucleus has a low breakup threshold ($S_p = 600$ keV) but since its ground state is usually deemed to consist of a proton in the $1d_{5/2}$ shell outside the doubly magic ^{16}O core it is not considered to constitute a halo due to the large centrifugal barrier. Rather, it is the low-lying $1/2^+$ first excited state (bounded by 105 keV) with the "valence" proton in the $2s_{1/2}$ shell which is thought to be a proton halo [19]. The inherent nuclear structure properties of ^{17}F, therefore, make it a prime candidate for reaction studies and for investigating the effect on the fusion cross section of a possible proton halo in a low-lying bound excited state rather than the ground state.

There have been several experimental studies using ^{17}F beams [9,20–28]. Among these studies, one measured the fusion-fission cross section for a ^{208}Pb target where it was concluded that at energies around the Coulomb barrier no enhancement of the fusion cross section is observed compared to those for the stable ^{19}F and the ^{16}O core with the same target [9], in contrast with the results for the $^{8}\mathrm{B}+^{58}\mathrm{Ni}$ system [17] but consistent with those for $^{8}\mathrm{B}+^{28}\mathrm{Si}$ [18]. It has been suggested that this lack of an enhancement in the fusion cross section could be due to an effective polarization of the ^{17}F in the strong Coulomb field of the ^{208}Pb target, leading to a shielding effect on the halo proton [29]. In a recent experiment where the reaction dynamics of the $^{17}\mathrm{F}+^{58}\mathrm{Ni}$ system was studied, it was found that the behavior of the total fusion cross section was identical with that of the $^{16}\mathrm{O}+^{58}\mathrm{Ni}$ system at above-barrier energies, but enhancement was observed below the Coulomb barrier which coupled discretized continuum channels (CDCC) calculations demonstrated was due to the effect of couplings to the $^{17}\mathrm{F}\rightarrow{}^{16}\mathrm{O}+p$ breakup process [28].

The present paper reports a measurement of the total fusion cross-section excitation function for the $^{17}\mathrm{F}+^{12}\mathrm{C}$ system at energies around the Coulomb barrier to search for the effects of its weak binding in a light mass system, thus, obviating any possible shielding effects and complementing the existing data sets for medium and heavy mass targets by extending the range of studies to a system where Coulomb effects should be minimal. A novel detector system developed at Florida State University allows for simultaneous detection of the incoming beam and the fusion products. The fusion products are measured simultaneously over an extended energy range without changing the energy of the incoming beam. The same experimental conditions were used to measure the fusion cross sections for the more tightly bound stable systems $^{16}\mathrm{O}+^{12}\mathrm{C}$ and $^{19}\mathrm{F}+^{12}\mathrm{C}$ at energies near the Coulomb barrier, thus, enabling a direct comparison of the fusion cross sections for all three systems.

II. EXPERIMENTAL DETAILS

The experiment was performed at the John D. Fox accelerator laboratory at Florida State University (FSU). A ^{17}F radioactive beam was produced by the RESOLUT radioactive beam facility [30]. A stable ^{16}O beam from the SNICS ion source was accelerated to 64.5 MeV by the tandem Van de Graaff accelerator and boosted to 91.5 MeV by the coupled LINAC accelerator. A liquid-nitrogen-cooled deuterium gas production target kept at a pressure of 350 torr was bombarded with the ^{16}O beam. The radioactive ^{17}F beam ($t_{1/2} = 64.5$ s) was produced at a rate of $\approx$600 particles per second (pps) in-flight via the $^{16}\mathrm{O}(d,n)\,^{17}\mathrm{F}$ reaction and focused onto the detector system by the superconducting solenoid of RESOLUT. The main contaminant was the primary ^{16}O beam at a rate of $\approx$1100 pps, which was used simultaneously in our experiment. A measurement with a stable ^{19}F beam from the tandem accelerator was also performed.

The 69.1-MeV ^{17}F beam and its main contaminant, the 58.1-MeV ^{16}O beam, were delivered to the *Encore* active-target detector. *Encore* is a multisampling ionization chamber recently developed at FSU, optimized to measure fusion cross sections with low-intensity exotic beams ($\leqslant$10 kHz). *Encore* is based on the MUSIC detector at Argonne National Laboratory (ANL) [31]. Details of the *Encore* detector will be published in a separate paper [32]. This detector system and analysis procedure has been successfully used at the ANL for measurements of fusion reactions with carbon isotopes [3] as well as for measurements of (α,p) and (α,n) reactions [33,34].

A schematic of the *Encore* detector is shown in the upper panel of Fig. 1. The beam enters through a 2.11-mg/cm^2 HAVAR window. *Encore* works as an ionization chamber with an electric field perpendicular to the beam axis. The detector is filled with gas which serves as both target and counting material. *Encore* measures energy losses as the beam passes through the detector. Ionization electrons produced by the interactions of the beam with the gas drift towards the segmented anode where the charge is collected, providing a signal proportional to the energy deposited by the ionizing particle.

After the beam enters the detector it travels 3 cm in a dead region before entering the segmented anode region. Energy losses of the beam are measured as it passes through the detector via 16 anode signals (strips $1, 2, \ldots, 16$) subdivided into left and right as shown in the lower panel of Fig. 1. The left and right halves of the 16 strips are independently read using two 16-channel MPR-16 preamplifiers connected with high-density FGG lemo cables and added together in the analysis. Two extra anode signals at the beginning and end of the detector (strips 0 and 17) are read individually and are used for vetoing and control. Signals from the cathode and the Frisch grid are also read out. For this experiment *Encore* was

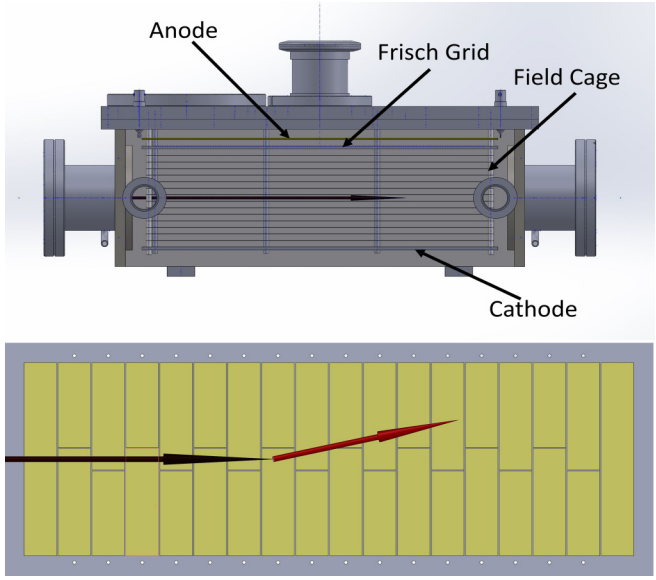

FIG. 1. Upper panel: Three-dimensional schematic of the *Encore* detector, a multisampling ionization chamber where the field cage produces a perpendicular electric field. The field cage consists of a negatively biased cathode, voltage divider wired planes, a Frisch grid, and a segmented anode. The beam passes through the center of the active region. Lower panel: Schematic of the segmented anode. The first and last strips are used as veto and control, respectively. The 16 strips subdivided into left and right halves are also shown. The black arrow indicates a beam particle entering the active region of the detector. A fusion reaction occurs in strip 7 creating an evaporation residue (red arrow) which is identified by its larger energy loss signal.

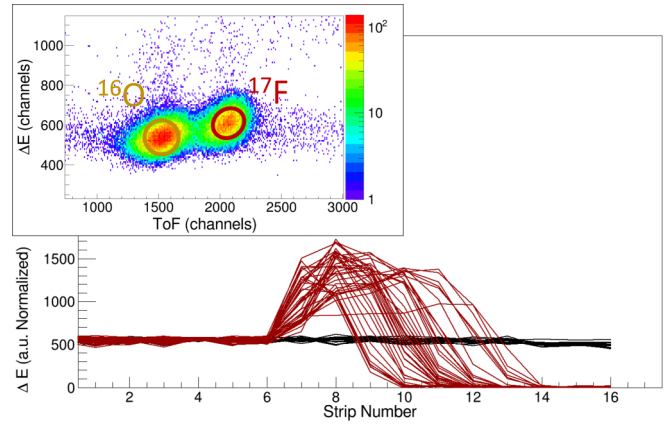

FIG. 2. Experimental traces measured in *Encore*. The beam traces inside the detector (black) have been normalized to a fixed value for the analysis. The normalization allows a consistent threshold to be set when searching for energy jumps within the segmented anode strips of the detector. Experimental $^{17}F + ^{12}C$ fusion events occurring in strip 7 are shown by the red traces. A jump in energy loss is seen as a result of the creation of an evaporation residue which will stop in the detector prior to the beam. The inset in the top-left corner shows the separation of the ^{17}F and ^{16}O beams in *Encore* due to their different time of flight.

filled with CH_4 gas at 168 torr. A gas handling system was used to recirculate the gas inside the detector. The pressure of the gas was constantly monitored by a pressure gauge. The value of the pressure of the gas in the detector remained constant within the precision of the gauge meter (0.5%) during the full measurement. The CH_4 gas used contains less than 1% of ^{13}C, therefore, any contribution from reactions with the ^{13}C in the gas is negligible. The gain of the anode segments was optimized to be more sensitive to signals corresponding to the interaction of the beam with the carbon in the CH_4 gas. Given the large difference in energy signals, the detector was not sensitive to the light particles or to interactions between the beam and the hydrogen in the gas.

The energy losses measured in each strip are analyzed on an event-by-event basis. One event through the detector, called a trace, is composed of 34 signals from the anode - 16 from the right side, 16 from the left side, 1 from strip 0 and 1 from strip 17. Most of the time *Encore* measures beamlike events. A sample of the experimental ^{17}F beam traces is shown by the black lines in Fig. 2 where they are normalized to channel 500 for the analysis.

Guided by energy loss simulations, an algorithm was developed to search for fusion reactions in the detector on an event-by-event basis. Fusionlike events are characterized by a beamlike trace followed by a sudden jump in the energy loss in the specific strip where the fusion reaction occurs due to the larger charge of the evaporation residue. The evaporation residue loses much more energy than the beam, therefore, the fusion trace stays high for a few strips before going to zero. Experimental fusion traces for the $^{17}F + ^{12}C$ system occurring in strip 7 are shown by the red lines in Fig. 2. The left and right segmentations of the anode provide multiplicity information which allows events, such as elastic and inelastic scatterings to be identified. Fusion events and beam events happen in either the right or the left side of the anode strips (multiplicity one), whereas scattering events have signals in both sides of the anode strips (multiplicity two) and can be easily rejected.

Encore provides full angular coverage of the evaporation residues allowing for a measurement of the total fusion cross section per strip. This translates into a measurement of the fusion excitation function of the system over a wide energy range using a single beam energy. The range of the excitation function is determined solely by the energy of the beam and the gas pressure in the detector. Since *Encore* measures all the beam all the time, it provides an absolute beam normalization of the measured total fusion cross sections. *Encore* is particularly efficient for fusion measurements with low-intensity exotic beams ($\leqslant$10 kHz) since there is no need to retune the energy of the beam to measure several points in an excitation function.

III. EXPERIMENTAL RESULTS

A silicon detector was mounted inside, at the end of the detector, for beam tuning purposes. Without gas in the detector and after the entrance HAVAR window, the energy of the ^{17}F beam was measured to be 61.2 MeV [full width at half maximum (FWHM) = 2 MeV] in the laboratory frame whereas that of the primary $^{16}O^{8+}$ beam was measured to be

TABLE I. Total fusion cross sections for the $^{17}F + ^{12}C$ system measured in the present experiment as a function of center-of-mass energy.

$E_{c.m.}$ (MeV)	σ (mb)
19.4 ± 0.5	914 ± 88
18.4 ± 0.5	797 ± 89
17.4 ± 0.5	728 ± 85
16.3 ± 0.5	789 ± 91
15.2 ± 0.5	831 ± 94
14.0 ± 0.6	704 ± 89
12.8 ± 0.6	660 ± 86
11.6 ± 0.6	516 ± 81
10.3 ± 0.6	240 ± 55
8.9 ± 0.7	150 ± 47

51.2 MeV (FWHM = 1.7 MeV). Once the detector was filled with gas, the ^{17}F and ^{16}O beams were separated in *Encore* by their different time of flights and their different ΔE signals as shown in the inset of Fig. 2.

In the present experiment the fusion excitation function of the $^{17}F + ^{12}C$ system was measured inside the active region of the detector over the range in the center-of-mass energy corresponding to $E_{c.m.} = 19.4 - 9.0$ MeV with an average energy of 1.2 MeV deposited in each strip. In order to extract the total fusion cross section per strip, the identified fusion events in a given strip are counted and normalized by the number of beam events in the detector. The corresponding energy and target thickness per strip, determined by the beam energy, gas pressure inside the detector, and size of the strip were calculated using LISE++ [35]. The study by Carnelli *et al.* [31] showed the validity of this approach. The error bars on the cross-section measurements are dominated by statistics. Systematic uncertainties are due to target thickness (i.e., the size of the anode strips, the pressure of the gas, and variations in temperature). A conservative minimum of 10% error bars on the cross sections has been adopted to account for systematic uncertainties. The error bars in energy arise from the 1.5-cm thickness of the strips and the possibility of the reaction occurring anywhere within the width of a particular strip. The error bars in the energy consider that the reaction occurred in the middle of the strip. The measured total fusion cross-section values are reported in Table I.

Fusion events from the primary ^{16}O beam were measured simultaneously in *Encore* with those for ^{17}F. The fusion cross sections for the $^{16}O + ^{12}C$ system, thus, obtained are plotted in Fig. 3 together with previous measurements from the literature [36–44]. The good agreement between the present $^{16}O + ^{12}C$ fusion data and the previous measurements gives confidence in the $^{17}F + ^{12}C$ fusion measurements.

In order to make a systematic comparison of any effects on the fusion cross section due to the exotic nature of ^{17}F, we also performed a measurement with its stable counterpart ^{19}F on a ^{12}C target. A 65-MeV ^{19}F beam at a rate of $\approx 1 \times 10^4$ pps was delivered to *Encore* which was filled with CH_4 gas at a pressure of 131 torr. This pressure was chosen to scan a similar range in center-of-mass energy to the $^{17}F + ^{12}C$ measurement.

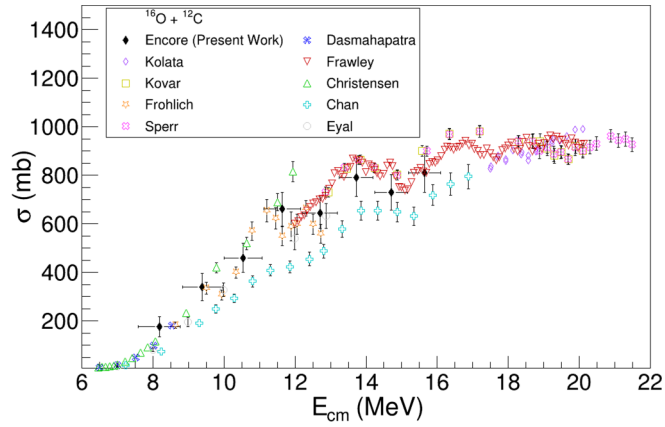

FIG. 3. Total fusion cross sections for $^{16}O + ^{12}C$ (black diamonds) measured in the present experiment compared with previously published data [36–44].

The ^{19}F arrived in the first control strip at 51 MeV, depositing between 0.75 and 1.2 MeV in each strip with an average of 0.9 MeV. The absolute cross sections for the $^{19}F + ^{12}C$ system in the energy range of $E_{c.m.} = 17.8 - 11$ MeV measured in this experiment are plotted in Fig. 4 together with previously published data [36,45,46]. The good agreement between the *Encore* measurements and the previous data confirms the consistency of our analysis procedure.

IV. ANALYSIS

One of the main issues when comparing fusion data for different interacting systems and, in particular, when addressing whether cross sections are enhanced or hindered, is the various ways that fusion data from different systems are presented and compared. Whereas various reduced units may be found in the literature [47–49], we have chosen to present our results using those defined by Gomes *et al.* [50] which eliminate the so-called "geometrical effects." These reduced units, also referred as the "simplified traditional method," are completely

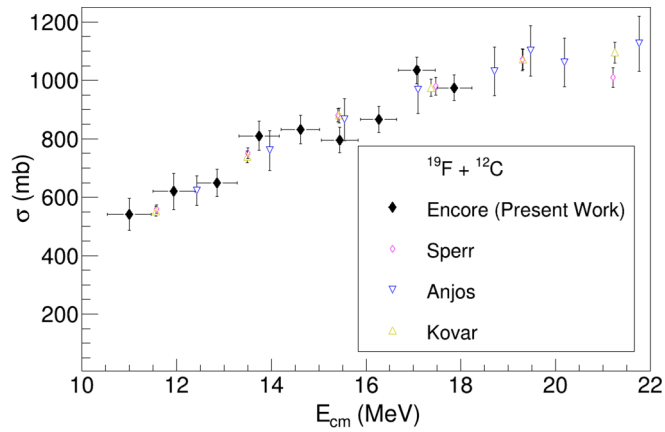

FIG. 4. Total fusion cross sections for $^{19}F + ^{12}C$ (black diamonds) measured in the present experiment compared with previously published data [36,45,46].

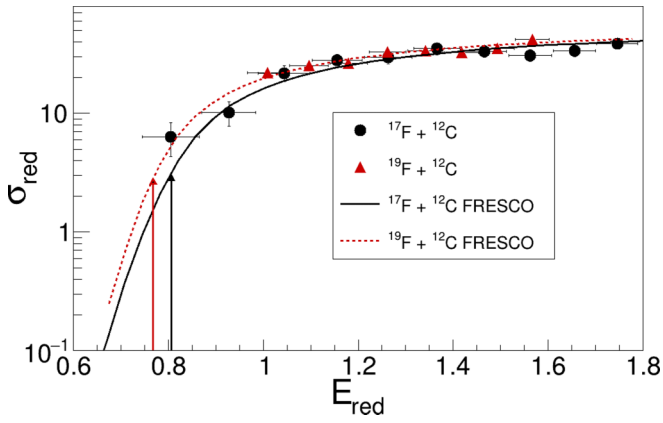

FIG. 5. Reduced total fusion cross sections for the $^{17}F + ^{12}C$ (black circles) and $^{19}F + ^{12}C$ (red triangles) systems measured in this paper. The corresponding no-coupling barrier penetration calculations using double-folded real potentials are denoted by the solid and dotted lines, respectively. The fusion barrier heights extracted from the potentials are indicated by the vertical arrows.

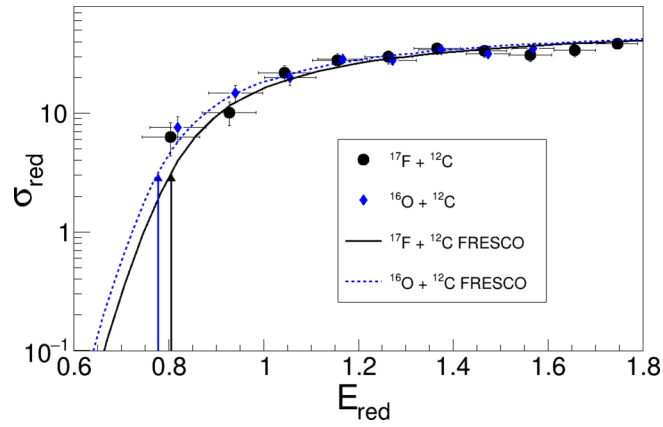

FIG. 6. Reduced total fusion cross sections for the $^{17}F + ^{12}C$ (black circles) and $^{16}O + ^{12}C$ (blue diamonds) systems measured in this paper. The corresponding no-coupling barrier penetration calculations using double-folded real potentials are denoted by the solid and dotted lines, respectively. The fusion barrier heights extracted from the potentials are indicated by the vertical arrows.

model independent and appropriate when used for systems of similar masses [7], such as those considered in this paper.

In this representation,

$$E_{red} = E_{c.m.}\left(A_p^{1/3} + A_t^{1/3}\right)/(Z_t Z_p), \quad (1)$$

and

$$\sigma_{red} = \sigma/\left(A_p^{1/3} + A_t^{1/3}\right)^2, \quad (2)$$

where $E_{c.m.}$ is the energy in the center-of-mass system in MeV, σ is the measured cross section in millibarns, and A_p, A_t, Z_p, and Z_t refer to the mass (A) and the nuclear charge (Z) of the projectile (p) and target (t) nuclei involved in the reaction.

In employing these reduced units we seek to minimize biases arising from "trivial" differences in Coulomb barrier heights and the $A^{1/3}$ nuclear radius variation which could "wash out" any structure effects that may be evident in the data [50] whereas at the same time retaining any "static" effects due to the increased size of the halo state. Using this convention, our measurements of the $^{17}F + ^{12}C$ fusion excitation function are plotted together with those for the $^{19}F + ^{12}C$ and $^{16}O + ^{12}C$ systems carried out under the same experimental conditions using the *Encore* detector at FSU in Figs. 5 and 6, respectively.

Also displayed in Figs. 5 and 6 are theoretical fusion excitation functions for the three systems calculated with the code FRESCO [51]. The real parts of the nuclear potentials were obtained using the double-folding procedure and the M3Y nucleon-nucleon interaction [52]. The ^{12}C, ^{16}O, and ^{19}F nuclear matter densities were derived from the experimental charge densities of Refs. [53–55], respectively, by unfolding the proton charge density and assuming that $\rho_{Nuc} = (1 + N/Z)\rho_p$. The ^{17}F nuclear matter density was taken from Ref. [56]. The double-folded potentials were calculated with the code DFPOT [57]. An imaginary potential of the Woods-Saxon squared form with parameters $W = 50$ MeV, $r = 1.0 \times (12^{1/3} + A_p^{1/3})$, $a = 0.3$ fm effectively reproduced the incoming-wave boundary condition, the total fusion cross section being calculated as the absorption by this potential. In all three systems it was found that no channel couplings were needed to reproduce the experimental results, which were well described by barrier penetration calculations [58]. The fusion barriers (V_b), fusion radii (R_b), and barrier curvatures ($\hbar\omega$) extracted from the double-folded potentials are given in Table II.

The measured total fusion cross sections for the $^{17}F + ^{12}C$ (black circles) and $^{19}F + ^{12}C$ (red triangles) systems plotted in Fig. 5 agree with each other well over the measured energy range when compared in reduced units. No enhancement or reduction of the ^{17}F fusion cross section compared with that for its stable counterpart is observed. The FRESCO calculations for both systems are also shown in Fig. 5 as solid and dotted lines for the $^{17}F + ^{12}C$ and $^{19}F + ^{12}C$ systems, respectively. The extracted barrier parameters for ^{17}F and ^{19}F are in close agreement, suggesting that the weak binding of ^{17}F and the possible proton-halo nature of its low-lying $1/2^+$ excited state have little or no influence on the fusion cross section in the measured energy range, in accord with previous results for the heavy $^{17}F + ^{208}Pb$ [9,22] and medium mass $^{17}F + ^{58}Ni$ [28] systems.

The total fusion cross sections for the $^{17}F + ^{12}C$ (black circles) and $^{16}O + ^{12}C$ (blue diamonds) systems are compared

TABLE II. Fusion barrier parameters for the systems studied in this paper extracted from the double-folded potentials used in the FRESCO calculations. When reduced according to the scheme of Gomes *et al.* [50] the barrier heights V_b for the three systems are almost identical: 0.78, 0.77, and 0.81 for $^{16}O + ^{12}C$, $^{19}F + ^{12}C$, and $^{17}F + ^{12}C$, respectively.

System	V_b (MeV)	R_b (fm)	R_b (fm)
$^{16}O + ^{12}C$	7.76	8.01	2.67
$^{19}F + ^{12}C$	8.37	8.36	2.56
$^{17}F + ^{12}C$	8.95	8.03	3.04

in Fig. 6. No enhancement or reduction of the ^{17}F fusion cross section compared to that for its ^{16}O core is observed when the excitation functions are plotted in reduced units. The FRESCO calculations for these two systems are also shown in Fig. 6 as the solid and dotted lines, respectively. The V_b values extracted for ^{17}F and ^{16}O are significantly different (see Table II) as expected due to their differing Z values. However, their reduced values 0.81 and 0.78, respectively, are almost identical, suggesting that the valence proton has little or no influence on the ^{17}F fusion cross section over the measured energy range. The R_b values are also similar: 8.03 and 8.01 fm, respectively, again suggesting that the valence proton has minimal influence on the fusion.

The lack of enhancement of the ^{17}F total fusion cross sections compared to those for its ^{16}O core is consistent with calculated values of the ground-state rms matter radius of ^{17}F which yield values similar to that of the ground state of ^{16}O (see, e.g., Ref. [59]). Although the rms radius of the ^{17}F 0.495 MeV $1/2^+$ excited state is significantly larger, commensurate with its proposed halo status, the lack of enhancement of the ^{17}F fusion cross section strongly suggests that its influence on the fusion process is small, either through coupling effects on the fusion barrier height or directly as a result of fusion of the ^{17}F after being excited to this state.

In order further to test this conclusion, coupled channel (CC) calculations were also performed with FRESCO. The "bare," no-coupling potential was the same as that used in the barrier penetration calculation described previously, the total fusion cross section in this case being calculated as the sum of the absorption by the Woods-Saxon squared imaginary potential in all channels.

Couplings to the 0.495-MeV $1/2^+$ state of ^{17}F and the 4.44-MeV 2^+ state of ^{12}C were included using standard collective model form factors. The $B(E2)$ for the ^{17}F coupling was taken from Ref. [60], and the nuclear deformation length was derived from this value assuming the collective model and a radius of $1.3 \times 17^{1/3}$ fm. The ^{12}C $B(E2)$ was taken from Ref. [61], and the nuclear deformation length was taken from Ref. [62].

It is possible to calculate the absorption by the imaginary potential for individual channels using FRESCO, equivalent to the fusion cross section in the model used here. In Fig. 7 we present the excitation functions for the total fusion and for each of the following channels: the entrance channel with both the ^{17}F projectile and the ^{12}C target in their respective ground states, ^{17}F in its 0.495-MeV $1/2^+$ excited state, ^{12}C in its ground state, ^{17}F in its ground state, and ^{12}C in its 4.44-MeV 2^+ excited state. Mutual excitation was not considered. The data are omitted for the sake of clarity, but they are well reproduced by the calculated total fusion excitation function.

The fusion excitation function obtained from the no-coupling calculation (not shown) is visually indistinguishable from the CC result on the scale of the figure down to values of $E_{red} = 0.75$, a slight enhancement due to the coupling being visible at lower energies. Careful comparison of the two calculations indicates that the coupling induces enhancement of the total fusion cross section below the Coulomb barrier and suppression above it, although the latter, in particular, is too small to be seen on a logarithmic plot. The coupling

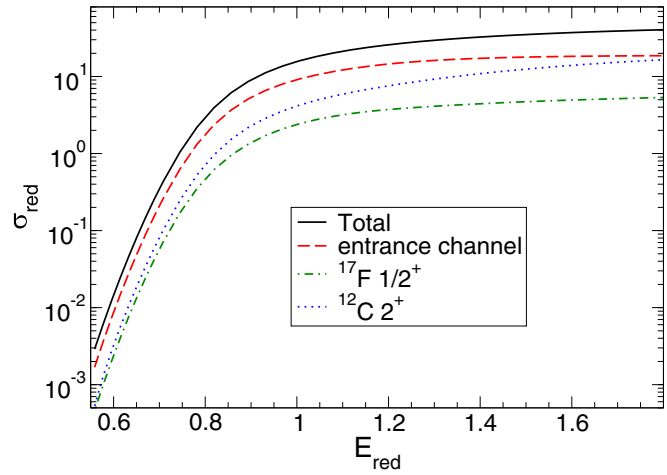

FIG. 7. Fusion excitation functions for ^{17}F + ^{12}C calculated using the code FRESCO. The solid curve denotes the total fusion cross section, the dashed curve fusion for the entrance channel (projectile and target in their respective ground states), the dot-dashed curve fusion for the channel with the ^{17}F in its 0.495-MeV $1/2^+$ excited state, the ^{12}C in its ground state, and the dotted curve fusion for the channel with ^{17}F in its ground state and ^{12}C in its 4.44-MeV 2^+ excited state.

effects of both the 0.495-MeV $1/2^+$ ^{17}F excited state and the 4.44-MeV 2^+ ^{12}C excited state on the fusion may, thus, be considered negligible over the measured energy range, confirming the conclusion of the barrier penetration calculation. In addition, the breakdown of the total fusion cross section into its individual channels shows that the contribution from fusion with ^{17}F in its 0.495-MeV $1/2^+$ excited state is small over the measured E_{red} range, being about an order of magnitude smaller than the total. By contrast, fusion with ^{12}C in its 4.44-MeV 2^+ excited state is much more important, becoming comparable to fusion from the entrance channel at the highest E_{red} values. The calculations predict that fusion with ^{17}F in its 0.495-MeV $1/2^+$ excited state becomes more important at subbarrier energies, but the trend suggests that it would only make a significant contribution to the total fusion in the relatively deep subbarrier region where the total fusion cross section is small, only becoming equal to fusion with ^{12}C in its 4.44-MeV 2^+ excited state at $E_{red} \approx 5.5$ where fusion from the entrance channel still dominates the total.

The calculations presented in Fig. 7 used the same double-folded real potential in all channels, calculated using the ^{17}F ground-state density of Ref. [56]. Thus, they do not take into account the extended size of the 0.495-MeV $1/2^+$ proton-halo state of ^{17}F. However, test calculations where the diagonal potential for the channel with ^{17}F in this state was recalculated using the appropriate ^{17}F matter density of Ref. [59] which explicitly includes the proton halo gave almost identical results.

V. DISCUSSION AND CONCLUSIONS

To summarize, an experimental campaign to study the influence of the structure of the weakly bound proton drip-line

nucleus ^{17}F on its total fusion cross section with ^{12}C was carried out using the *Encore* active-target detector system at FSU. *Encore* measures energy losses as the beam travels through the detector using a segmented anode. The total fusion excitation function over a wide energy range can be measured with absolute normalization and without changing the beam energy. Systematic measurements with its stable counterparts ^{16}O and ^{19}F were also performed under the same experimental conditions.

The comparison of the data in reduced units presented in this paper indicates no special influence on the total fusion cross section over the measured energy range due to the specific structure of ^{17}F, in particular, the proton-halo nature of its its low-lying first excited state, confirming previous findings for the heavy $^{17}F + ^{208}Pb$ [9] and medium mass $^{17}F + ^{58}Ni$ [28] systems. The lack of a fusion enhancement in the present paper with the low-Z target nucleus ^{12}C provides a further test of the proposal by He *et al.* [29] that in the $^{17}F + ^{208}Pb$ system no enhancement in the fusion cross section was observed because the large Coulomb field of the ^{208}Pb target polarizes ^{17}F such that the proton follows the ^{16}O core in its interaction with the target. Together with the results for the $^{17}F + ^{58}Ni$ [28] system the present paper suggests that, at least, for incident energies down to the top of the Coulomb barrier, a polarization effect of this type cannot account for the lack of enhancement in the total fusion cross section for ^{17}F since the charge products of the systems analyzed now extend from 738 through 252 down to 54 and no enhancement is observed.

Coupled-channel calculations showed that the influence of coupling to the ^{17}F proton-halo state on the total fusion cross section for the $^{17}F + ^{12}C$ system was suppression above the barrier and enhancement below (with respect to the no-coupling calculation) although the size of the effect was negligible except for energies $E_{red} < 0.7$. The CC calculations further indicated that fusion from the channel with ^{17}F propagating in the halo state makes only a small contribution to the total fusion. Thus, the halo nature of the 0.495-MeV $1/2^+$ excited state of ^{17}F is seen to have little or no influence on the total fusion in the energy range studied here, explaining the similarity of the fusion cross sections for the ^{17}F, ^{19}F, and $^{16}O + ^{12}C$ systems when plotted in reduced units.

Analogous CC calculations performed for the $^{17}F + ^{58}Ni$ and ^{208}Pb systems showed qualitatively similar behavior in that the coupling to the 0.495-MeV $1/2^+$ excited state of ^{17}F induced enhancement of the total fusion cross section below the Coulomb barrier and suppression above, albeit the coupling effects were more important and increased with increasing target charge, a well attested effect. The coupling effect is consistent with that seen in the CDCC calculations for the $^{17}F + ^{58}Ni$ system [28]. The breakdown of the total fusion cross section by channels showed that the contribution from the channel with the ^{17}F propagating in its 0.495-MeV $1/2^+$ excited state was again small for both systems.

Taking the results for the $^{17}F + ^{12}C$, $^{17}F + ^{58}Ni$, and $^{17}F + ^{208}Pb$ systems all together we see a consistent picture emerging. By far the most important influence of the ^{17}F 0.495-MeV $1/2^+$ excited state on the total fusion is via its coupling effect on the fusion barrier, and the size of this effect scales with increasing target charge as for any inelastic coupling. The main influence of the halo nature of this state on the total fusion cross section will, thus, only be indirectly via any impact it may have on the coupling strength linking it to the ground state. Our final conclusion is, therefore, that as regards the total fusion, ^{17}F essentially behaves in a similar way to any other nucleus with strongly coupled excited states, neither its weak binding nor the halo nature of its first excited state making any striking impact on this observable.

The self-normalizing and efficient capabilities of the *Encore* detector make it an ideal system systematically to study the fusion cross sections for other proposed proton-halo nuclei: ^{8}B [17,18], ^{17}Ne [63], and ^{27}P [64] and, thus, determine whether there are any specific structure related effect on the total fusion cross section for these nuclei at energies near the top of the Coulomb barrier. Other "detector targets," such as Ne, Ar, Kr, and Xe could be used further to explore the Z dependence of the fusion cross sections for exotic proton-halo nuclei.

ACKNOWLEDGMENTS

This work was supported by the National Science Foundation under Grants No. PHY-1712953 and No. PHY-2012522 and by the State of Florida.

[1] B. B. Back, H. Esbensen, C. L. Jiang, and K. E. Rehm, Recent developments in heavy-ion fusion reactions, Rev. Mod. Phys. **86**, 317 (2014).

[2] C. L. Jiang, D. Santiago-Gonzalez, S. Almaraz-Calderon, K. E. Rehm, B. B. Back, K. Auranen, M. L. Avila, A. D. Ayangeakaa, S. Bottoni, M. P. Carpenter, C. Dickerson, B. DiGiovine, J. P. Greene, C. R. Hoffman, R. V. F. Janssens, B. P. Kay, S. A. Kuvin, T. Lauritsen, R. C. Pardo, J. Sethi *et al.* Reaction rate for carbon burning in massive stars, Phys. Rev. C **97**, 012801 (2018).

[3] P. F. F. Carnelli, S. Almaraz-Calderon, K. E. Rehm, M. Albers, M. Alcorta, P. F. Bertone, B. Digiovine, H. Esbensen, J. O. Fernández Niello, D. Henderson, C. L. Jiang, J. Lai, S. T. Marley, O. Nusair, T. Palchan-Hazan, R. C. Pardo, M. Paul, and C. Ugalde, Measurements of Fusion Reactions of Low-Intensity Radioactive Carbon Beams on ^{12}C and Their Implications for the Understanding of X-Ray Bursts, Phys. Rev. Lett. **112**, 192701 (2014).

[4] N. Keeley, R. Raabe, N. Alamanos, and J. L. Sida, Fusion and direct reactions of halo nuclei at energies around the coulomb barrier, Prog. Part. Nucl. Phys. **59**, 579 (2007).

[5] I. Tanihata, H. Hamagaki, O. Hashimoto, Y. Shida, N. Yoshikawa, K. Sugimoto, O. Yamakawa, T. Kobayashi, and N. Takahashi, Measurements of Interaction Cross Sections and Nuclear Radii in the Light *p*-Shell Region, Phys. Rev. Lett. **55**, 2676 (1985).

[6] I. Tanihata, H. Hamagaki, O. Hashimoto, S. Nagamiya, Y. Shida, N. Yoshikawa, O. Yamakawa, K. Sugimoto, T. Kobayashi, D. E. Greiner, N. Takahashi, and Y. Nojiri, Measurements of interaction cross sections and radii of he isotopes, Phys. Lett. B **160**, 380 (1985).

[7] L. F. Canto, P. R. S. Gomes, R. Donangelo, J. Lubian, and M. S. Hussein, Recent developments in fusion and direct reactions with weakly bound nuclei, Phys. Rep. **596**, 1 (2015).

[8] A. B. Balantekin and N. Takigawa, Quantum tunneling in nuclear fusion, Rev. Mod. Phys. **70**, 77 (1998).

[9] K. E. Rehm, H. Esbensen, C. L. Jiang, B. B. Back, F. Borasi, B. Harss, R. V. F. Janssens, V. Nanal, J. Nolen, R. C. Pardo, M. Paul, P. Reiter, R. E. Segel, A. Sonzogni, J. Uusitalo, and A. H. Wuosmaa, Fusion Cross Sections for the Proton Drip Line Nucleus ^{17}F at Energies Below the Coulomb Barrier, Phys. Rev. Lett. **81**, 3341 (1998).

[10] J. J. Kolata, V. Guimarães, and E. F. Aguilera, Elastic scattering, fusion, and breakup of light exotic nuclei, Eur. Phys. J. A **52**, 123 (2016).

[11] V. Scuderi, A. Di Pietro, P. Figuera, M. Fisichella, F. Amorini, C. Angulo, G. Cardella, E. Casarejos, M. Lattuada, M. Milin, A. Musumarra, M. Papa, M. G. Pellegriti, R. Raabe, F. Rizzo, N. Skukan, D. Torresi, and M. Zadro, Fusion and direct reactions for the system ^{6}He + ^{64}Zn at and below the coulomb barrier, Phys. Rev. C **84**, 064604 (2011).

[12] V. V. Parkar, G. Marquinez, I. Martel, A. M. Sánchez-Benítez, L. Acosta, R. Berjillos, J. Dueñas, J. L. Flores, J. P. Bolívar, A. Padilla, M. A. G. Alvarez, D. Beaumel, M. J. G. Borge, A. Chbihi, C. Cruz, M. Cubero, J. P. Fernandez Garcia, B. Fernández Martínez, J. Gomez Camacho, N. Keeley, J. A. Labrador, M. Marquis, M. Mazzocco *et al.*, Fusion of 8he with 206pb around coulomb barrier energies, EPJ Web Conf. **17**, 16009 (2011).

[13] A. M. Vinodkumar, W. Loveland, R. Yanez, M. Leonard, L. Yao, P. Bricault, M. Dombsky, P. Kunz, J. Lassen, A. C. Morton, D. Ottewell, D. Preddy, and M. Trinczek, Interaction of ^{11}Li with ^{208}Pb, Phys. Rev. C **87**, 044603 (2013).

[14] C. Signorini, A. Yoshida, Y. Watanabe, D. Pierroutsakou, L. Stroe, T. Fukuda, M. Mazzocco, N. Fukuda, Y. Mizoi, M. Ishihara, H. Sakurai, A. Diaz-Torres, and K. Hagino, Subbarrier fusion in the systems ^{11,10}Be + ^{209}Bi, Nuc. Phys. A **735**, 329 (2004).

[15] D. J. Hinde and M. Dasgupta, Systematic analysis of above-barrier fusion of ^{9,10,11}Be + ^{209}Bi, Phys. Rev. C **81**, 064611 (2010).

[16] P. G. Hansen, A. S. Jensen, and B. Jonson, Nuclear halos, Annu. Rev. Nucl. Part. Sci. **45**, 591 (1995).

[17] E. F. Aguilera, P. Amador-Valenzuela, E. Martinez-Quiroz, D. Lizcano, P. Rosales, H. García-Martínez, A. Gómez-Camacho, J. J. Kolata, A. Roberts, L. O. Lamm, G. Rogachev, V. Guimarães, F. D. Becchetti, A. Villano, M. Ojaruega, M. Febbraro, Y. Chen, H. Jiang, P. A. DeYoung, G. F. Peaslee *et al.*, Near-Barrier Fusion of the ^{8}B + ^{58}Ni Proton-Halo System, Phys. Rev. Lett. **107**, 092701 (2011).

[18] A. Pakou, E. Stiliaris, D. Pierroutsakou, N. Alamanos, A. Boiano, C. Boiano, D. Filipescu, T. Glodariu, J. Grebosz, A. Guglielmetti, M. La Commara, M. Mazzocco, C. Parascandolo, K. Rusek, A. M. Sánchez-Benítez, C. Signorini, O. Sgouros, F. Soramel, V. Soukeras *et al.*, Fusion cross sections of ^{8}B + ^{28}Si at near-barrier energies, Phys. Rev. C **87**, 014619 (2013).

[19] R. Morlock, R. Kunz, A. Mayer, M. Jaeger, A. Müller, J. W. Hammer, P. Mohr, H. Oberhummer, G. Staudt, and V. Kölle, Halo Properties of the First $1/2^{+}$ State in ^{17}F from the ^{16}O (p, γ) ^{17}F Reaction, Phys. Rev. Lett. **79**, 3837 (1997).

[20] J. F. Liang *et al.*, Dynamic polarization in the coulomb breakup of loosely bound ^{17}F, Phys. Lett. B **681**, 22 (2009).

[21] Q. Wang, J.-L. Han, Z.-G. Xiao, H.-S. Xu, Z.-Y. Sun, Z.-G.Hu, X.-Y. Zhang, H.-W. Wang, R.-S. Mao, X.-H. Yuan, Z.-G. Xu, T.-C. Zhao, H.-B. Zhang, H.-G. Xu, H.-R. Qi, Y. Wang, F. Jia, L.-J. Wu, X.-L. Ding, Q. Gao *et al.*, Exotic behaviour of angular dispersion of weakly bound nucleus ^{17}F at small angles, Chin. Phys. Lett. **23**, 1731 (2006) .

[22] G. L. Zhang, C. L. Zhang, H. Q. Zhang, C. J. Lin, D. Y. Pang, X. K. Wu, H. M. Jia, G. P. An, Z. D. Wu, X. X. Xu, F. Yang, Z. H. Liu, S. Kubono, H. Yamaguchi, S. Hayakawa, D. N. Binh, Y. K. Kwon, N. Iwasa, M. Mazzocco, M. La Commara *et al.*, Quasi-elastic scattering of the proton drip line nucleus ^{17}F on ^{12}C at 60 mev, Eur. Phys. J. A **48**, 65 (2012).

[23] M. Mazzocco, C. Signorini, D. Pierroutsakou, T. Glodariu, A. Boiano, C. Boiano, F. Farinon, P. Figuera, D. Filipescu, L. Fortunato, A. Guglielmetti, G. Inglima, M. La Commara, M. Lattuada, P. Lotti, C. Mazzocchi, P. Molini, A. Musumarra, A. Pakou, C. Parascandolo *et al.*, Reaction dynamics for the system ^{17}F + ^{58}Ni at near-barrier energies, Phys. Rev. C **82**, 054604 (2010).

[24] J. F. Liang, J. R. Beene, H. Esbensen, A. Galindo-Uribarri, J. Gomez del Campo, C. J. Gross, M. L. Halbert, P. E. Mueller, D. Shapira, D. W. Stracener, and R. L. Varner, Breakup of weakly bound ^{17}f well above the coulomb barrier, Phys. Lett. B **491**, 23 (2000).

[25] J. F. Liang, J. R. Beene, A. Galindo-Uribarri, J. Gomez del Campo, C. J. Gross, P. A. Hausladen, P. E. Mueller, D. Shapira, D. W. Stracener, R. L. Varner, J. D. Bierman, H. Esbensen, and Y. Larochelle, Breakup of ^{17}F on ^{208}Pb near the coulomb barrier, Phys. Rev. C **67**, 044603 (2003).

[26] C. Signorini, D. Pierroutsakou, B. Martin, M. Mazzocco, T. Glodariu, R. Bonetti, A. Guglielmetti, M. La Commara, M. Romoli, M. Sandoli, E. Vardaci, H. Esbensen, F. Farinon, P. Molini, C. Parascandolo, F. Soramel, S. Sidortchuk, and L. Stroe, Interaction of ^{17}F with a ^{208}Pb target below the coulomb barrier, Eur. Phys. J. A **44**, 63 (2010).

[27] M. Romoli, E. Vardaci, M. Di Pietro, A. De Francesco, A. De Rosa, G. Inglima, M. La Commara, B. Martin, D. Pierroutsakou, M. Sandoli, M. Mazzocco, T. Glodariu, P. Scopel, C. Signorini, R. Bonetti, A. Guglielmetti, F. Soramel, L. Stroe, J. Greene, A. Heinz *et al.*, Measurements of ^{17}F scattering by ^{208}Pb with a new type of large solid angle detector array, Phys. Rev. C **69**, 064614 (2004).

[28] L. Yang, C. J. Lin, H. Yamaguchi, J. Lei, P. W. Wen, M. Mazzocco, N. R. Ma, L. J. Sun, D. X. Wang, G. X. Zhang, K. Abe, S. M. Cha, K. Y. Chae, A. Diaz-Torres, J. L. Ferreira, S. Hayakawa, H. M. Jia, D. Kahl, A. Kim, M. S. Kwag *et al.*, Insight into the reaction dynamics of proton drip-line nuclear system ^{17}F + ^{58}Ni at near-barrier energies, Phys. Lett. B **813**, 136045 (2021).

[29] X. y. He, Q. Dong, and L. Ou, Shielding effects in fusion reactions with a proton-halo nucleus, Chin. Phys. C **44**, 054108 (2020).

[30] I. Wiedenhöver, L. T. Baby, D. Santiago-Gonzalez, A. Rojas, J. C. Blackmon, G. V. Rogachev, J. Belarge, E. Koshchiy, A. N. Kuchera, L. E. Linhardt, J. Lail, K. T. Macon, M. Matos, and

B. C. Rascol, Studies of exotic nuclei at the resolut facility of florida state university, in *Fission and Properties of Neutron-Rich Nuclei*, edited by J. H. Hamilton and A. V. Ramayya, Proceedings of the Fifth International Conference on ICFN5, Sanibel Island, FL, 2014 (World Scientific, Singapore, 2014), pp. 144–151.

[31] P. F. F. Carnelli, S. Almaraz-Calderon, K. E. Rehm, M. Albers, M. Alcorta, P. F. Bertone, B. Digiovine, H. Esbensen, J. Fernández Niello, D. Henderson, C. L. Jiang, J. Lai, S. T. Marley, O. Nusair, T. Palchan-Hazan, R. C. Pardo, M. Paul, and C. Ugalde, Multi-sampling ionization chamber (music) for measurements of fusion reactions with radioactive beams, Nucl. Instrum. Methods Phys. Res., Sect. A, Accelerators, Spectrometers, Detectors and Associated Equipment **799**, 197 (2015).

[32] B. W. Asher, S. Almaraz-Calderon, L. T. Baby, N. Gerken, E. Lopez-Saavedra, A. B. Morelock, and J. F. Perello, The Encore active target detector: a Multi-Sampling Ionization Chamber (unpublished).

[33] M. L. Avila, K. E. Rehm, S. Almaraz-Calderon, A. D. Ayangeakaa, C. Dickerson, C. R. Hoffman, C. L. Jiang, B. P. Kay, J. Lai, O. Nusair, R. C. Pardo, D. Santiago-Gonzalez, R. Talwar, and C. Ugalde, Experimental study of the astrophysically important $^{23}Na(\alpha, p)^{26}Mg$ and $^{23}Na(\alpha, n)^{26}Al$ reactions, Phys. Rev. C **94**, 065804 (2016).

[34] R. Talwar, M. J. Bojazi, P. Mohr, K. Auranen, M. L. Avila, A. D. Ayangeakaa, J. Harker, C. R. Hoffman, C. L. Jiang, S. A. Kuvin, B. S. Meyer, K. E. Rehm, D. Santiago-Gonzalez, J. Sethi, C. Ugalde, and J. R. Winkelbauer, Experimental study of $^{38}Ar + \alpha$ reaction cross sections relevant to the ^{41}Ca abundance in the solar system, Phys. Rev. C **97**, 055801 (2018).

[35] O. B. Tarasov and D. Bazin, Lise++: Radioactive beam production with in-flight separators, Nucl. Instrum. Methods Phys. Res., Sect. B **266**, 4657 (2008).

[36] D. G. Kovar, D. F. Geesaman, T. H. Braid, Y. Eisen, W. Henning, T. R. Ophel, M. Paul, K. E. Rehm, S. J. Sanders, P. Sperr, J. P. Schiffer, S. L. Tabor, S. Vigdor, B. Zeidman, and F. W. Prosser, Systematics of carbon- and oxygen-induced fusion on nuclei with $12 \leqslant a \leqslant 19$, Phys. Rev. C **20**, 1305 (1979).

[37] J. J. Kolata, R. M. Freeman, F. Haas, B. Heusch, and A. Gallmann, On the fusion cross section for $^{16}O + ^{12}C$, Phys. Lett. B **65**, 333 (1976).

[38] H. Fröhlich, P. Dück, W. Galster, W. Treu, H. Voit, H. Witt, W. Kühn, and S. M. Lee, Oscillations in the excitation function for complete fusion of $^{16}O + ^{12}C$ at low energies, Phys. Lett. B **64**, 408 (1976).

[39] Y.-D. Chan, H. Bohn, R. Vandenbosch, K. G. Bernhardt, J. G. Cramer, R. Sielemann, and L. Green, Gross structure in γ-ray yields following the $^{16}O\,^{12}C$ reaction, Nuc. Phys. A **303**, 500 (1978).

[40] P. Sperr, S. Vigdor, Y. Eisen, W. Henning, D. G. Kovar, T. R. Ophel, and B. Zeidman, Oscillations in the Excitation Function for Complete Fusion of $^{16}O + ^{12}C$, Phys. Rev. Lett. **36**, 405 (1976).

[41] B. Dasmahapatra, B. Čujec, and F. Lahlou, Fusion cross sections for $^{16}O + ^{13}C$ at low energies, Nucl. Phys. A **394**, 301 (1983).

[42] A. D. Frawley, N. R. Fletcher, and L. C. Dennis, Resonances in the $^{16}O + ^{12}C$ fusion cross section between $E_{c.m.} = 12$ and 20 MeV, Phys. Rev. C **25**, 860 (1982).

[43] P. R. Christensen, Z. E. Switkowskiw, and R. A. Dayras, Subbarrier fusion measurements for $^{12}C + ^{16}O$, Nucl. Phys. A **280**, 189 (1977).

[44] Y. Eyal, M. Beckerman, R. Chechik, Z. Fraenkel, and H. Stocker, Nuclear size and boundary effects on the fusion barrier of oxygen with carbon, Phys. Rev. C **13**, 1527 (1976).

[45] R. M. Anjos, V. Guimares, N. Added, N. Carlin Filho, M. M. Coimbra, L. Fante, M. C. S. Figueira, E. M. Szanto, C. F. Tenreiro, and A. Szanto de Toledo, Effect of the entrance channel mass asymmetry on the limitation of light heavy-ion fusion cross sections, Phys. Rev. C **42**, 354 (1990).

[46] P. Sperr, T. H. Braid, Y. Eisen, D. G. Kovar, F. W. Prosser, J. P. Schiffer, S. L. Tabor, and S. Vigdor, Fusion Cross Sections of Light Heavy-Ion Systems: Resonances and Shell Effects, Phys. Rev. Lett. **37**, 321 (1976).

[47] L. F. Canto, P. R. S. Gomes, J. Lubian, L. C. Chamon, and E. Crema, Disentangling static and dynamic effects of low breakup threshold in fusion reactions, J. Phys. G: Nucl. Part. Phys. **36**, 015109 (2008).

[48] L. F. Canto, P. R. S. Gomes, J. Lubian, L. C. Chamon, and E. Crema, Dynamic effects of breakup on fusion reactions of weakly bound nuclei, Nuc. Phys. A **821**, 51 (2009).

[49] J. M. B. Shorto, P. R. S. Gomes, J. Lubian, L. F. Canto, S. Mukherjee, and L. C. Chamon, Reaction functions for weakly bound systems, Phys. Lett. B **678**, 77 (2009).

[50] P. R. S. Gomes, J. Lubian, I. Padron, and R. M. Anjos, Uncertainties in the comparison of fusion and reaction cross sections of different systems involving weakly bound nuclei, Phys. Rev. C **71**, 017601 (2005).

[51] I. J. Thompson, Coupled reaction channels calculations in nuclear physics, Comput. Phys. Rep. **7**, 167 (1988).

[52] G. R. Satchler and W. G. Love, Folding model potentials from realistic interactions for heavy-ion scattering, Phys. Rep. **55**, 183 (1979).

[53] L. S. Cardman, J. W. Lightbody, S. Penner, S. P. Fivozinsky, X. K. Maruyama, W. P. Trower, and S. E. Williamson, The charge distribution of 12c, Phys. Lett. B **91**, 203 (1980).

[54] H. De Vries, C. W. De Jager, and C. De Vries, Nuclear charge-density-distribution parameters from elastic electron scattering, At. Data Nucl. Data Tables **36**, 495 (1987).

[55] P. L. Hallowell, W. Bertozzi, J. Heisenberg, S. Kowalski, X. Maruyama, C. P. Sargent, W. Turchinetz, C. F. Williamson, S. P. Fivozinsky, J. W. Lightbody, and S. Penner, Electron scattering from ^{19}F and ^{40}Ca, Phys. Rev. C **7**, 1396 (1973).

[56] R. Capote, M. Herman, P. Obložinský, P. G. Young, S. Goriely, T. Belgya, A. V. Ignatyuk, A. J. Koning, S. Hilaire, V. A. Plujko, M. Avrigeanu, O. Bersillon, M. B. Chadwick, T. Fukahori, Z.g Ge, Y. Han, S. Kailas, J. Kopecky, V. M. Maslov, G. Reffo *et al.*, Ripl–reference input parameter library for calculation of nuclear reactions and nuclear data evaluations, Nucl. Data Sheets **110**, 3107 (2009), Special Issue on Nuclear Reaction Data.

[57] J. Cook, Dfpot - a program for the calculation of double folded potentials, Comput. Phys. Commun. **25**, 125 (1982).

[58] C. Y. Wong, Interaction Barrier in Charged-Particle Nuclear Reactions, Phys. Rev. Lett. **31**, 766 (1973).

[59] H.-Y. Zhang, W.-Q. Shen, Z.-Z. Ren, Y.-G. Ma, J.-G. Chen, X.-Z. Cai, Z.-H. Lu, C. Chen, W. Guo, Y.-B. Wei, X.-F. Zhou, G.-L. Ma, and K. Wang, Structures of ^{17}F and ^{17}O, ^{17}Ne and ^{17}N in the ground state and the first excited state, Chin. Phys. Lett. **20**, 1462 (2003).

[60] C. A. Bertulani, G. Cardella, M. De Napoli, G. Raciti, and E. Rapisarda, Coulomb excitation of unstable nuclei at intermediate energies, Phys. Lett. B **650**, 233 (2007).

[61] S. Raman, C. W. Nestor, and P. Tikkanen, Transition probability from the ground to the first-excited 2+ state of even-even nuclides, At. Data Nucl. Data Tables **78**, 1 (2001).

[62] N. Keeley, K. W. Kemper, and K. Rusek, Strong multistep interference effects in ^{12}C(d, p) to the $9/2^+_1$ state in ^{13}C, Phys. Rev. C **92**, 054618 (2015).

[63] K. Tanaka, M. Fukuda, M. Mihara, M. Takechi, D. Nishimura, T. Chinda, T. Sumikama, S. Kudo, K. Matsuta, T. Minamisono, T. Suzuki, T. Ohtsubo, T. Izumikawa, S. Momota, T. Yamaguchi, T. Onishi, A. Ozawa, I. Tanihata, and T. Zheng, Density distribution of ^{17}Ne and possible shell-structure change in the proton-rich *sd*-shell nuclei, Phys. Rev. C **82**, 044309 (2010).

[64] D. Q. Fang, W. Q. Shen, J. Feng, X. Z. Cai, H. Y. Zhang, Y. G. Ma, C. Zhong, Z. Y. Zhu, W. Z. Jiang, W. L. Zhan, Z. Y. Guo, G. Q. Xiao, J. S. Wang, J. Q. Wang, J. X. Li, M. Wang, J. F. Wang, Z. J. Ning, Q. J. Wang, and Z. Q. Chen, Evidence for a proton halo in ^{27}P through measurements of reaction cross-sections at intermediate energies, Eur. Phys. J. A **12**, 335 (2001).